Establishment of an Integrated Italy–Malta Cross–Border System of Civil Protection. Geophysical Aspects
ISBN 978-88-548-8256-0
DOI 10.4399/97888548825604
pag. 31–45 (october 2015)

II. Overview of the seismic hazard in the Sicily channel archipelagos

Panzera F., D'Amico S., Lombardo G., Galea P., Akinci A.

1. Introduction

A joint Italo–Maltese research project (Costituzione di un Sistema Integrato di Protezione Civile Transfrontaliero Italo–Maltese, SIMIT) was financially supported by the European community. One of the aims of SIMIT was to improve the geological and geophysical information in Lampedusa and in Malta and ultimately to mitigate natural hazards. Although this region lies on the Sicily Channel Rift Zone, a seismically active domain of Central Mediterranean, the knowledge about seismotectonic and seismic hazard is not satisfactory. At present, seismic hazard assessment (SHA) for Italy (MPS Working Group, 2004), Tunisia (Ksentini and Romdhane, 2014) and more generally for whole European areas (Giardini *et al.*, 2013) do exist, whereas no specific SHA for the Sicily channel archipelagos are available. The Sicily Channel appears to be a region of moderate seismic activity, with the seismicity mainly located in the surrounding areas (Fig. 1). For the Malta archipelago a first catalogue, listing historical and felt earthquakes, was made by Galea (2007), whereas the *Database Macrosismico Italiano* (DBMI11; Locati *et al.*, 2011) does not list any data as regards earthquakes felt in Lampedusa. For this reason, in the present study, a theoretical seismic history was derived (Fig. 2) for Lampedusa and Malta, using the European–Mediterranean Earthquake Catalogue (EMEC) (Grünthal and Wahlström, 2012) and the attenuation relationship for macroseismic intensity data by Pasolini *et al.* (2008). The two study areas do not appear to have been affected by strong earthquakes occurring in the Sicily channel, but they were somehow struck by major earthquakes occurring in the surrounding area. Although the present description seems to exclude large shaking effects, SHA for the study region is

currently of primary interest for the near–future development of industrial and touristic facilities. The SHA can be performed using either a deterministic (DSHA) or a probabilistic (PSHA) approach. The DSHA uses individual earthquake sources and single–valued events to set up a specific scenario that describes the hazard. Typically, a seismic source location, an earthquake of specified size and a ground motion attenuation relationship are required. However, this approach does not provide information on the occurrence probability of an earthquake parameter (acceleration, magnitude) during a finite period of time (e.g., the useful lifetime of a particular structure or facility). PSHA, being a statistical approach, needs to identify a suitable time interval having good completeness of information. On the other hand, PSHA allows us to estimate the probability that an intensity parameter (e.g., peak ground acceleration) could exceed a defined value during a given time (e.g., 50 years) (McGuire, 2004). Such an approach accounts for all possible combinations of magnitude–location of shocks and models describing the effects and the occurrence rate of all earthquakes that could affect an area. In the present study we show the preliminary PSHA results for Lampedusa and the Maltese islands in terms of Peak Ground Acceleration (PGA) and Spectral Acceleration (SA) at different periods. Seismic hazard was computed through the Esteva–Cornell (1968) approach, which represents the widely utilized probabilistic method, using the CRISIS2015 code (Ordaz *et al.*, 2015).

2. Seismotectonic features and seismogenic sources

The Western Mediterranean area is characterized by a complex tectonic setting linked to the slow oblique plate convergence taking place between the Africa and Eurasia plates (Fig. 3a). Several seismotectonic models have been proposed but, the Africa-Eurasia plate boundary is still mostly represented through a simplified compressive lineament starting from Morocco and reaching Sicily (Serpelloni *et al.*, 2007). In this context the proposed seismic Source Zones (SZ) model, depicted in Figure 3b, is the output obtained by assembling the information coming from the source zone (SZ) model proposed for the SHA of the Italian territory (Meletti *et al.*, 2008) and the SHARE (Seismic Hazard Harmonization in Europe) model (Giardini *et al.*, 2013).

Going from North to South of the studied area the following source zones can be described. In the Tyrrhenian basin, located at the back of the Apennines and Sicilian–Maghrebian chains, we considered the SZ1, which takes into account the shallow seismicity of the NE Cal-

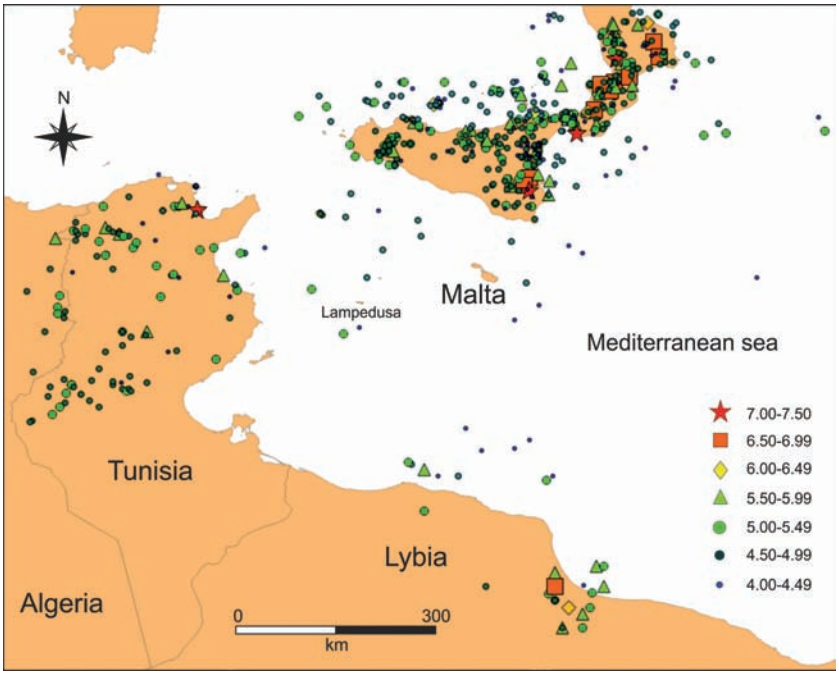

Figure 1. Main historical earthquake location for South–eastern Mediterranean area using EMEC data (1000–2006).

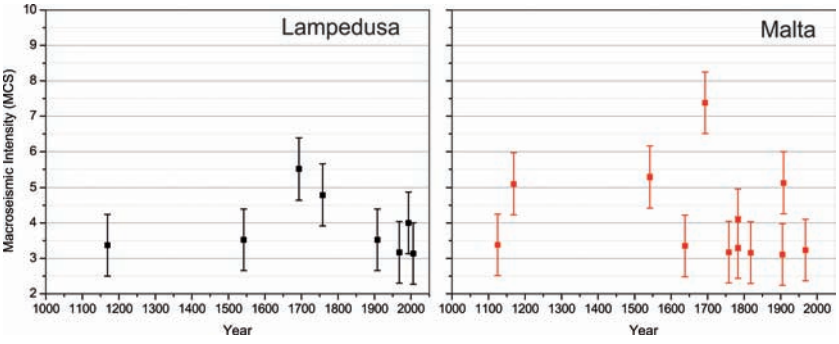

Figure 2. Theoretical seismic site histories for Lampedusa (left panel) and Malta (right panel) islands.

abria fore–arc. The SZ2 is linked to the transfer faults accompanying the slab retreat beneath the Calabrian Arc and the SZ3 that includes the seismicity related to the North Sicily offshore (Fig. 3a and b). All these SZ's are characterized by moderate earthquakes that can reach a moment magnitude (M_W) 5.5–6.0 (Fig. 1). As concerns Calabria, two important source zones are considered, SZ4 and SZ5. They are elongated transversally to the displacement direction of the Calabrian Arc and parallel to the Tyrrhenian and Ionian coasts extensional regimes (Monaco and Tortorici, 2000). In the two considered zones some of the strongest earthquakes that struck the Italian territory, such as the sequences of 1783, 1905 and 1908 (Rovida *et al.*, 2011), are located. In the northern boundary of Sicily, the compressional and transpressional

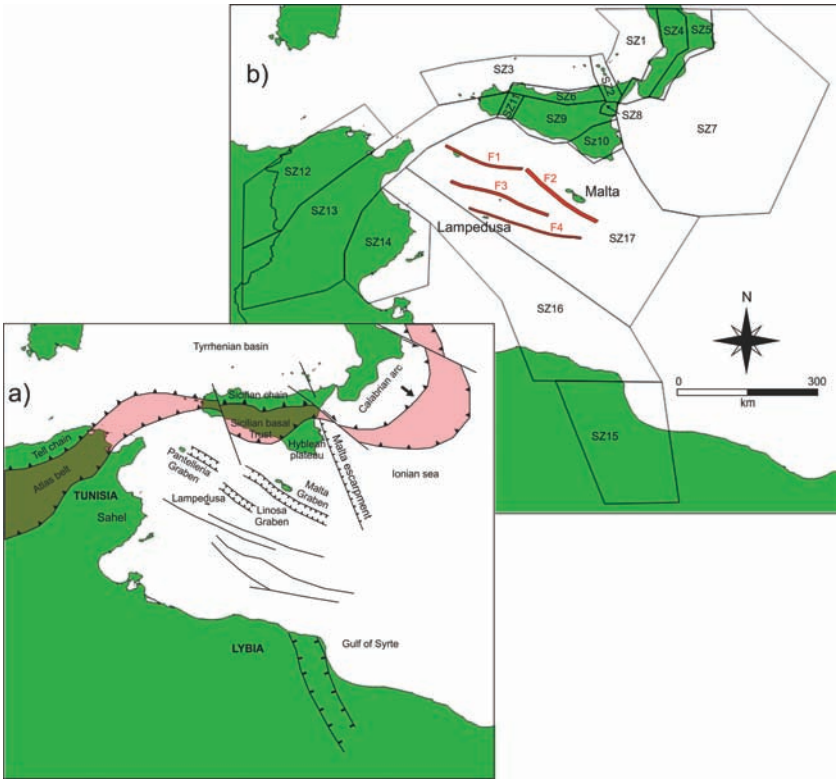

Figure 3. a) Simplified tectonic sketch of the study area with major structural domains; pink regions refer to trench areas. b) Source zone models considered for the PSHA with the Esteva–Cornell method.

faults linked to the Sicilian–Maghrebian chains, are enclosed in the SZ6. The SZ7, which reproduce another SHARE background SZ (Giardini *et al.*, 2013), delimits the Ionian area, taking into account the SE emplacement of the Calabria fore–arc which grows toward the Ionian Basin. The SZ8 refers to Mt. Etna volcano, characterized by seismogenic features totally different from the other parts of Sicily. Seismogenic faulting is here extremely shallow, which may cause surface faulting even for very moderate earthquakes (magnitude 5; e.g. Azzaro, 1999; Panzera *et al.*, 2011). The SZ9 is linked to the Sicilian basal thrust plane of the southward-verging Sicilian fold–and–thrust belt. It emerges along the Sciacca–Gela–Catania front and deepens northward reaching a depth of about 30 km. This SZ should be considered as a reasonable seismogenic source in mainland and central–southern Sicily (La Vecchia *et al.*, 2007). Two other important SZs round up the remaining seismogenic sources in Sicily. The first is the SZ10 where the major historical Sicilian earthquakes, all having intensity ranging between VI and XI on the MCS scale (Rovida *et al.*, 2011), took place. It has however to be specified that the identification of the causative faults of such events is still unclear and different hypotheses have been reported in literature (e.g. Argnani and Bonazzi, 2005; Gutscher *et al.*, 2006; Basili *et al.*, 2008). The second one is the SZ11, known as Belice, where the January 13th 1968 sequence (Mw 6.1) was located (Monaco *et al.*, 1996). The Strait of Sicily interrupts the continuity of the northern Africa seismic belt but, following the observations coming from the European Database of Seismogenic Faults (Basili *et al.*, 2013), we considered in our model the SZ12 and the SZ13. These zones include the seismicity linked both to the Tell domain and the Atlas foreland domain, respectively. The first being a thrust sheet that moved southeastward mainly during middle Miocene, and the second representing a complex fold belt of northern Tunisia (Masrouhi *et al.*, 2014). In Tunisia we considered also the SZ14 that it is part of the eastern Tunisia and Pelagean platform extending to the offshore domain. It is limited to the W and to the NW by the NS fold axis that represents an important feature of the Tunisian geology which was interpreted as a deep and old structure separating the Tunisian Atlas from the Sahel and Pelagean domain (Mourabit *et al.* 2014). As concerns Lybia, only the seismicity related to the NW–SE extensional fault of the Syrte basin was taken into account, therefore considering

the SZ15 (see Fig. 3b). Moreover, the SZ16 and SZ17 were drawn in order to enclose the Sicily channel seismicity. The SZ16 is indeed a link to the WNW–ESE strike–slip system and to the NNW–SSE grabens, that extends from the Pelagian Shelf to the Syrte Gulf and the Libya onshore (Serpelloni *et al.*, 2007), whereas the SZ17 takes in all the seismicity linked to the Pantelleria, Malta and Linosa grabens.

In addition to the source zones model previously described, we used also a combined model based on SZ and fault sources (FZ). In this second model, inside the SZ17, four fault sources (Fig. 3b) were considered as well. The geometric parameters associated to such faults (FZ) were taken from the European Database of Seismogenic Faults (EDSF) (Basili *et al.*, 2013). These faults are probably linked to the transtensional tectonics of the Sicily Channel.

3. Esteva–Cornell method

An SHA based on the Esteva–Cornell method, was performed using the open source code CRISIS2015. Such code requires as input data a source–zones model where both the seismic rate of each considered zone and a ground motion predictive equation are described. According to current international conventions for SHA (SSHAC, 1997), a logic tree approach was followed to consider and evaluate the epistemic uncertainties that affect the hazard estimates (Fig. 4). Special care was devoted to define alternative source–zone models to take into account the possibility of different seismogenic sources. This allowed us to take into account the uncertainties in the source location and in the fault mechanisms of the major earthquakes of the area. Following the considerations expressed in the previous section, a model combining both SZ and FZ approaches was therefore considered (see Figs. 3b and 4). The Gutenberg–Richter b–value coefficients and the seismic rates (λ) were computed using EMEC catalog (Grünthal and Wahlström, 2012). The maximum moment magnitude (M_w), as well as the seismogenic depth (H) and the faulting style, were taken from the literature.

Three ground–motion predictive equations were selected AB14 (Abrahamson *et al.*, 2014), BO14 (Boore *et al.*, 2014) and CB14 (Cambell and Borzogna, 2014).

In such equations, the earthquakes used to calibrate them are derived from tectonically active crustal regions such as California,

Taiwan, Japan, China, Alaska and the Mediterranean region (Italy, Greece, Turkey). In particular, for BO14 and CB14, the authors considered the possibility of adopting correction factors for the variations in the regional ground motion parameters. All these equations calculate different shaking parameters (PGA, PGV, SA), using the M_W, the Joyner–Boore source distance (R_{JB}), the closest distance to rupture area (R_{RUP}), the characteristic style–of–faulting and the site class. In our computation rock conditions ($V_{S,30} \geq 760$ m/s) were assumed.

An important assumption pertains to the site–to-source distance, especially for the disaggregation analysis. The disaggregation is here used to compute the contributions to the 10% exceedance probability in 50 years of PGA. In the adopted attenuation laws the distance was measured with R_{JB}, whereas the SZ definition was done referring to epicentral locations. In the CRISIS2015 code, the attenuation relationships can be specified in terms of 4 different measures of distance such as the focal, the epicentral, the R_{JB} or R_{RUP}. If the R_{RUP} or the R_{JB}distances are used, CRISIS2015 needs to know the rupture area or the rupture length, as a function of magnitude, in order to compute the required distances. The code then assumes that the relation be-

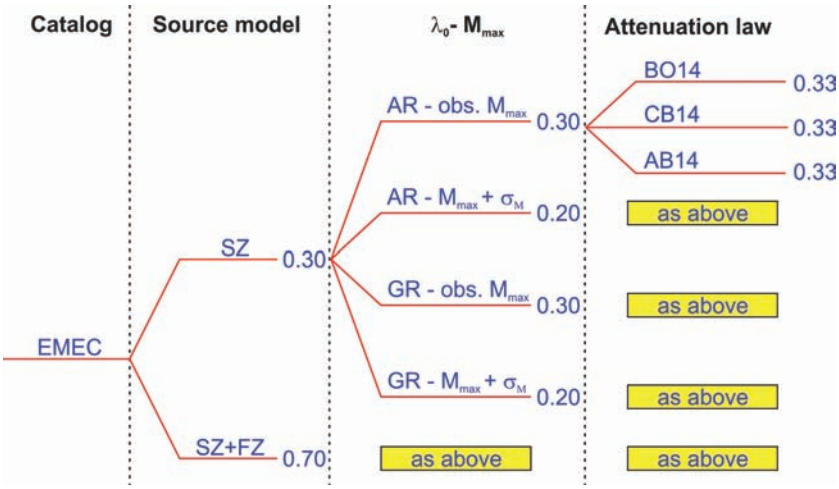

Figure 4. Logic tree used for the hazard computation.

tween area/rupture length and magnitude is: $A=K_1e^{k_2M}$; $L=K_3e^{k_4M}$, where A is the source area (in km²), L is the rupture length (in km), M stands for the magnitude and K_1, K_2, K_3 and K_4 are constants given by the user or chosen from a built-in set of constants. In this study, source area (A) and the Wells and Coppersmith (1994) constants were adopted, specifying these latter in the "source geometry" screen of the code. In such instances, CRISIS2015 will assume that the earthquake takes place in a plane defined by the source geometry, and that the rupture area is a circle within this plane with an area A and a radius

$$r = \sqrt{\frac{A}{\pi}} \tag{1}$$

The CRISIS 2015 code uses the type of distance adopted in the attenuation relationship for the hazard computation and, in addition, in the "global parameter" screen, it allows us to specify which kind of distance the users would like to adopt for the disaggregation output. According to this possibility, we preferred to express the results of the disaggregation in terms of epicentral distance.

3.1. *Activity rate, b–value and maximum magnitude*

For most of the seismic sources used in this study the seismicity is described by the equation:

$$\lambda(M) = \lambda_{min}\frac{e^{-\beta M} - e^{-\beta M_{max}}}{e^{-\beta M_{min}} - e^{-\beta M_{max}}} \quad M_{min} \leq M \leq M_{max} \tag{2}$$

where λ_{min}, is the seismicity rate associated to M_{min} (minimum considered magnitude) β is equal to b–value of the Gutenberg–Richter multiplied by 2.3 and M_{max} is the maximum magnitude.

These parameters are estimated, for each SZ, by means of EMEC catalog and a statistical approach based on the use of activity rates (AR). The AR values were obtained by dividing the number of seismic events of each magnitude class (eight of 0.4 M_W with minimum magnitude equal 4.0), by the completeness time. Then the parameters of Gutenberg–Richter, were obtained by interpolating the Log(AR) values, of each magnitude class, with a least square method (see examples in Figure 5).

Table 1. Magnitude classes and completeness time intervals used in this study for the SR1 and SR2 areas obtained from TCEF plots.

Magnitude class	SR1	SR2
$4.0 \leq M < 4.4$	1980–2006	1970–2006
$4.4 \leq M < 4.8$	1920–2006	1870–2006
$4.8 \leq M < 5.2$	1920–2006	1870–2006
$5.2 \leq M < 5.6$	1900–2006	1800–2006
$5.6 \leq M < 6.0$	1900–2006	1700–2006
$6.0 \leq M < 6.4$	1700–2006	1700–2006
$6.4 \leq M < 6.8$	1700–2006	1400–2006
$6.8 \leq M < 7.2$	1700–2006	1100–2006

As concerns the completeness time, the Temporal Course of Earthquake Frequency method (TCEF) was applied to the declustered catalog. The aftershocks and foreshocks were removed from the catalog using the method proposed by Grünthal (1985). It has to be remembered that the EMEC catalog includes several events belonging to the CPTI04 catalog which is already declustered. Such events were therefore excluded from the declustering procedure and considered as main shocks. Plots of the cumulative number of events pertaining to each magnitude class vs. time were eventually drawn (Fig. 6).

Since in the studied area, the information about historical earthquakes is not homogeneous, to better identify the periods of completeness, it was preferred to split the catalog into two sub–regions SR1 and SR2. The first includes SZ12, SA13, SZ14, SZ15, SZ16 whereas the second takes in all remaining SZ (see Tab. 1 and Fig. 6). The com-

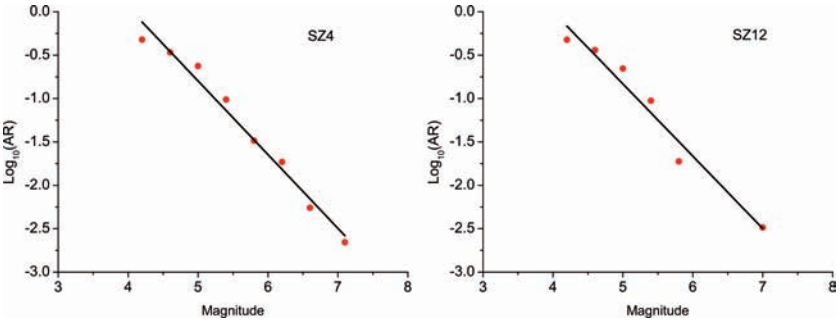

Figure 5. Examples of Gutenberg–Richter estimation using magnitude vs. Log(AR).

Table 2. Parameters used in seismic hazard computation.

Id	M_{min}	↓=b*ln(10)	λ_{GR}	λ_{AR}	M_{max}	H (km)	FM
SZ1	4.2	2.587	0.337	0.270	5.8±0.3	13	Normal
SZ2	4.2	1.937	0.307	0.214	6.1±0.3	11	Strike slip
SZ3	4.2	2.317	0.384	0.200	6.0±0.3	13	Reverse
SZ4	4.2	1.956	0.759	0.479	7.1±0.3	11	Normal
SZ5	4.2	2.004	0.282	0.216	6.9±0.3	11	Unspecified
SZ6	4.2	2.307	0.338	0.196	5.9±0.3	9	Reverse
SZ7	4.2	2.784	0.331	0.257	5.6±0.3	13	Reverse
SZ8	4.2	3.005	0.185	0.147	5.2±0.3	4	Unspecified
SZ9	4.2	2.409	0.234	0.174	6.0±0.3	13	Reverse
SZ10	4.2	1.603	0.149	0.155	7.4±0.3	13	Strike slip
SZ11	4.6	1.614	0.051	0.050	6.3±0.3	9	Reverse
SZ12	4.2	1.918	0.685	0.477	7.0±0.3	13	Reverse
SZ13	4.6	2.929	0.493	0.331	5.8±0.3	13	Reverse
SZ14	4.6	1.651	0.072	0.065	5.8±0.3	13	Reverse
SZ15	4.2	1.250	0.143	0.109	6.9±0.3	13	Normal
SZ16	4.2	2.040	0.338	0.274	5.7±0.3	13	Strike slip
SZ17	4.2	1.925	0.178	0.172	4.8±0.3	13	Strike slip

pleteness levels were therefore derived by observing in these graphs evident slope changes (see Fig. 6). It is indeed commonly assumed that the most recent slope change occurs when the data become complete for each magnitude class (Gasperini and Ferrari, 2000). It is important to remember that the completeness time of a magnitude class cannot be later than that of a smaller magnitude class in the same area. For this reason, when this occurs the completeness time of the smaller magnitudes was assigned also to the greater one.

In Tab. 2 the parameters achieved for each SZ are listed:

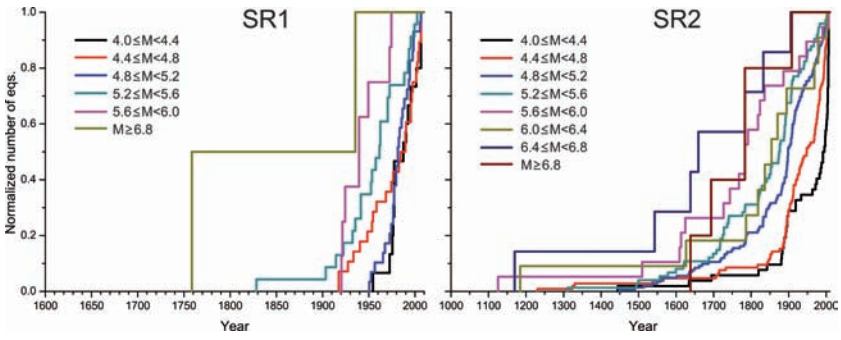

Figure 6. TCEF plots for the two considered sub–regions.

— Minimum magnitude (M_{min}) considered in the computation for each seismic zone;
— β value, seismicity rate from Gutenberg–Richter (λ_{GR}) and Activity rate (λ_{AR}) for the M_{min};
— Observed historical maximum magnitude (M_{max}) for each seismic zone and corresponding uncertainties considered in historical magnitudes (σ_M);
— Depth of the seismogenic layer H (km);
— Fault mechanism (FM).

The procedure used to obtain σ_M consists in computing the mean, modal and median values of the magnitude standard deviations listed in the EMEC catalog. The magnitude standard deviations range between 0.07 and 0.62, with a mean and median values of 0.26. For this reason a σ_M equal to 0.3 was chosen in the hazard computation.

3.2. *Fault sources and characteristic earthquake*

The earthquake catalogue for the Sicily Channel only spans over a short time interval, therefore information about the seismicity associated with the most important seismogenic faults can be different from that instrumentally observed. For this reason, a characteristic earthquake approach was applied to the above considered SZs, taking into account the Sicily Channel faults (F1, F2, F3 and F4 in Figure 3b) reported in the European Database of Seismogenic Faults (EDSF; Basili *et al.*, 2013). The seismicity of these seismogenic faults could be described through the following equation:

$$\lambda(M) = \lambda_{min} \frac{\phi\left[\frac{M_{max}-E(M)}{\sigma}\right] - \phi\left[\frac{M-E(M)}{\sigma}\right]}{\phi\left[\frac{M_{max}-E(M)}{\sigma}\right] - \phi\left[\frac{M_{min}-E(M)}{\sigma}\right]} \quad M_{min} \leq M \leq M_{max} \quad (3)$$

where $E(M)$ is the expected characteristic earthquake magnitude, σ is the magnitude standard deviation and ϕ is the normal standard distribution function (Ordaz *et al.*, 2015).

To attain the parameters linked to each fault it was assumed that the seismic activity is a process of energy accumulation and release and

consequently the seismic moment is a measure of the earthquake size in terms of the energy released. The characteristic seismic moment accumulation/release model agrees with the energy balance principle and assumes that the moment released by an earthquake is equal to the accumulation along a seismic fault during a recurrence interval (Ren and Zhang, 2013). Then, if the seismic moment upper bound (M_0 in Nm) of a seismic fault is known as well as its related annual moment rate (in Nm/yr), the recurrence time interval of a characteristic earthquake can be estimated as:

$$T = M_0 \equiv M_0 = \frac{M_0}{\mu LWD} \tag{4}$$

where D is the slip rate, μ is the shear modulus considered equal to 3×10^{10} Nm^{-2}, L and W are respectively the segment length and the down-dip width of the fault (see details in Tab. 3). To estimate the seismic moment upper bound the relationship proposed by Leonard (2010 and 2012) was used:

$$\log M_0 = \frac{15}{4}\log W - \frac{9}{4}\log C_1 + \log C_2\mu \tag{5}$$

where C_1 and C_2 are regression constants for the intraplate strike–slip faults (Leonard, 2010; 2012). The corresponding moment magnitude (M_w) was computed using the relation proposed by Kanamori and Brodsky (2004):

$$M_w = \frac{\log M_0}{1.5} \tag{6}$$

4. Results and discussion

Seismic hazard, using the Esteva–Cornell approach, was computed for each branch of the logic tree considering rock conditions ($V_{S,30}$=760 m/s) and 10% exceedance probability in 50 years. Figure 7 shows the hazard maps for the Sicily channel in terms of PGA and SA evaluated at 0.2, 0.5 and 1.0 s.

It is interesting to observe that Lampedusa has a slightly higher hazard than the Malta archipelago. Such findings are, in our opinion,

Table 3. Parameters associated with the considered seismogenic faults taken from EDSF and computed using formulas (4), (5) and (6). E(M) denotes the expected earthquake.

	Id	Depth (km)		Strike (deg)	Dip (deg)	Rake (deg)	$\dot{D}$ (mm/y)	L (km)	W (km)
		min	max						
From EDSF	F1	4	12	90-120	50-70	190-240	0.2-0.5	150	10
	F2	3	15	120-140	50-75	190-240	0.2-0.5	175	14
	F3	4	13	110-130	50-70	190-240	0.2-0.5	193	11
	F4	3	13	275-300	60-80	190-230	0.3-0.8	216	11

	Id	$\dot{M}$ (Nm/yr) x 10^{16}			M_o (Nm) x 10^{19}			M_w	Return period
		min	max	E(M)	min	max	E(M)	E(M)	$T_{E(M)}$
Computed	F1	0.9	2.3	1.4	0.2	0.3	0.3	6.2±0.4	176
	F2	1.5	3.7	2.3	0.7	1.1	0.9	6.6±0.4	381
	F3	1.3	3.2	2.0	0.3	0.5	0.4	6.3±0.4	178
	F4	2.1	5.7	3.5	0.3	0.5	0.4	6.3±0.4	103

significantly affected by the location of the considered islands with respect to the used seismic zones. Lampedusa is indeed placed very close to the SZ16 and F4 that have a higher seismicity rate with respect to the SZ17 and F2. The choice of the source zone model for Sicily channel seems then to significantly affect the hazard computation. As matter of fact the b–value and the activity rates (λ) of SZ16 are slightly higher than those obtained for the SZ17. Moreover, considering the parameters associated with the F4 seismogenic fault, located slightly north of Lampedusa, this structure appears as the most hazardous fault segment of the Sicily channel. However, it is evident that as the spectral period increases (see Fig. 7), the difference in seismic hazard between the two areas decreases. As suggested by Tselentis *et al.* (2010) such effect is linked to the magnitude of large events that mainly affects the long periods (>0.5 s) of SA whereas, small magnitude events mostly influence the short–period section of the spectrum.

A two dimensional disaggregation in magnitude and epicentral distance (R_{epi}) was also performed for 475 years return time. Such procedure allows us to identify the design earthquake that characterizes the local seismic hazard. Similarly to the procedure used for obtaining the hazard maps, the disaggregation charts (Fig. 8) were obtained for the

whole logic tree. Inspection of the disaggregation graphs (Fig. 8) shows that the major contribution to the dominant scenario for PGA is given by an earthquake having magnitude ranging between 4.20–4.84 and epicentral distance less than 30 km, both for Lampedusa and Malta.

The higher value of PGA of the Lampedusa island can be explained in terms of the disaggregation chart which shows a significant contribution to the hazard of earthquakes having magnitude 5.16-5.80 and distance less than 60 km. This evidence, probably linked to the SZ16, is not observed in the Malta disaggregation chart. On the other hand, if we consider long periods (SA = 1.0 s), the hazard of Malta archipelago increases as a consequence of large earthquakes (Mw≥7.0) having distance in the range 120–180 km. In the Lampedusa disaggregation chart, the contribution of these events is however present but their distance increases (240–300 km).

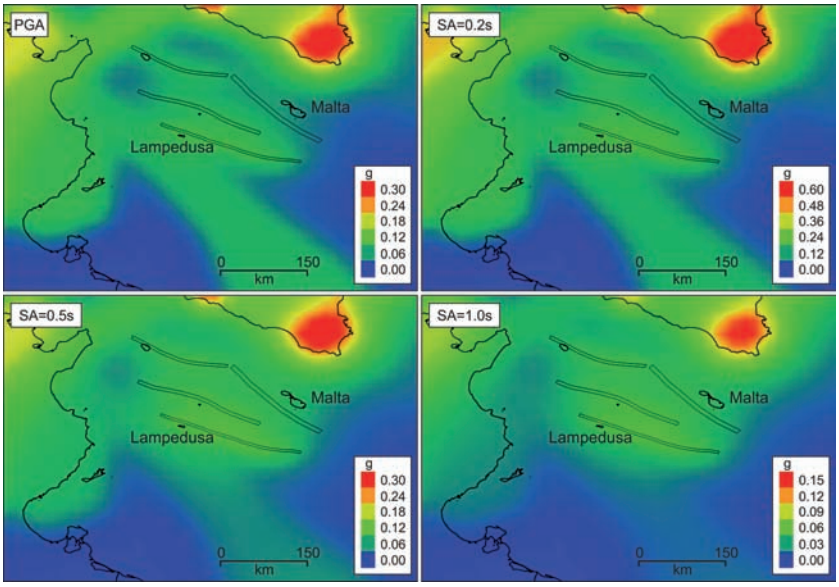

Figure 7. Hazard maps of the investigated area for Peak Ground Acceleration (PGA) and Spectral Acceleration (SA) at different periods.

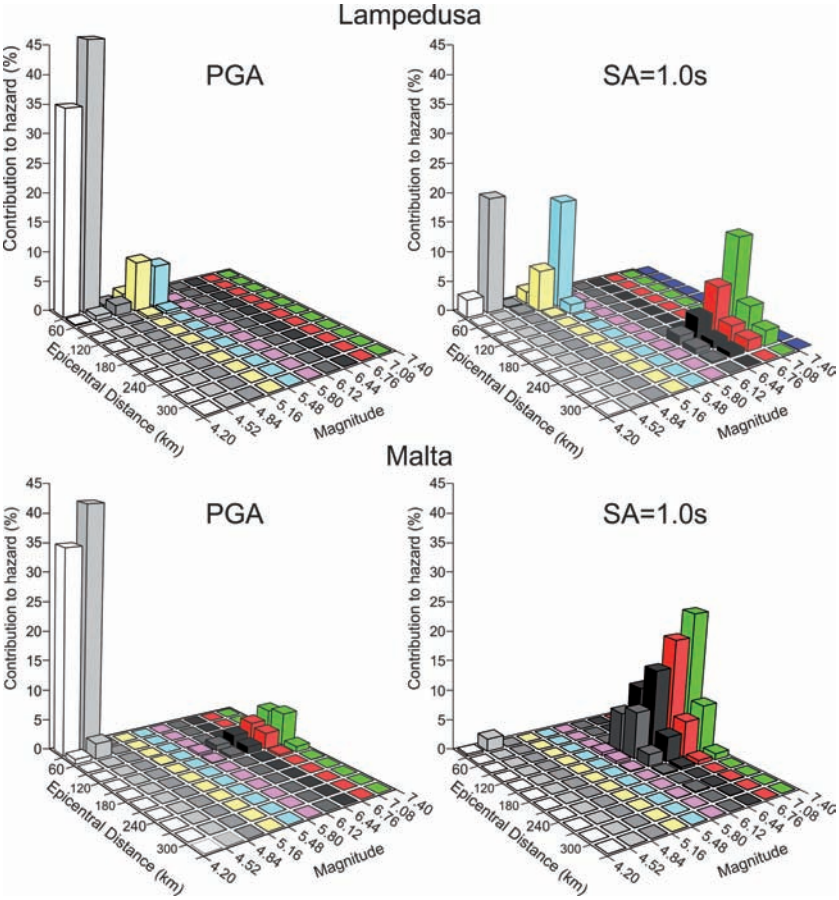

Figure 8. Disaggregation charts for Lampedusa and Malta archipelago, in terms of Peak Ground Acceleration (PGA) and Spectral Acceleration (SA) at periods of 1.0 s.

Panzera F.[1], D'Amico S.[2], Lombardo G.[1], Galea P.[2], Akinci A.[3]

1. Dipartimento di Scienze Biologiche, Geologiche e Ambientali, Università di Catania, Italy. Corresponding author: Panzera F., fpanzera@unict.it.

2. Department of Geosciences (previously at Physics Department), University of Malta, Msida, Malta.

3. Istituto Nazionale di Geofisica e Vulcanologia, Sez. Sismologia e Tettonofisica, Roma, Italy.